Recognition of Muscle Fatigue Status Based on Improved Wavelet Threshold and CNN-SVM

JUNHONG WANG[ID][1,2]**, YINING SUN**[1,2]**, AND SHAOMING SUN**[2,3]
[1]Hefei Institutes of Physical Science, Chinese Academy of Sciences, Hefei 230031, China
[2]Hefei Institutes of Physical Science, University of Science and Technology of China, Hefei 230026, China
[3]Chinese Academy of Sciences Institute of Technology Innovation, Hefei 230088, China
Corresponding author: Yining Sun (ynsun@iim.cas.cn)

ABSTRACT This study proposed a muscle fatigue classification method based on surface electromyography (sEMG) signals to achieve accurate muscle fatigue detection and classification. A total of 20 healthy young participants (14 men and 6 women) were recruited for fatigue testing on a cycle ergometer, and sEMG signals and oxygen uptake were recorded during the test. First, the measured sEMG signals were denoised with an improved wavelet threshold method. Second, the V-slope method was used to identify the ventilation threshold (VT) to reflect the muscle fatigue state. The time- and frequency-domain features of the sEMG signals were extracted, including root mean square, integrated electromyography, median frequency, mean power frequency, and band spectral entropy. Third, the time- and frequency-domain features of the sEMG signals were labeled either ''normal'' or ''fatigued'' based on the VT. Finally, the statistical features of 16 participants were selected as the training data set of the Convolutional Neural Network–Support Vector Machine (CNN-SVM), Support Vector Machine, Convolutional Neural Network, and Particle Swarm Optimization–Support Vector Machine algorithms. In addition, the statistical features of the four remaining participants were used as the test data set to analyze the classification accuracy of the four aforementioned algorithms. Experimental results indicated that the denoising effect of the improved wavelet threshold algorithm proposed in this study was satisfactory. The CNN-SVM algorithm achieved accurate muscle fatigue classification and 80.33%–86.69% classification accuracy.

INDEX TERMS Convolutional neural network-support vector machine (CNN-SVM), muscle fatigue, sEMG, wavelet threshold.

I. INTRODUCTION

The muscular system is an important part of the human body, providing power to the body's movements. Exercise-induced muscle fatigue refers to the physiological phenomenon when the maximum voluntary contraction force of a muscle is caused by exercise or a temporary decline in the output power [1]. When muscles are fatigued for long periods during exercise, the risk of athletic injury increases. Therefore, the accurate detection of muscle fatigue is the basis for muscle fatigue relief and treatment and has important kinematics and medical significance. Electromyographic (EMG) signals are recorded by placing an EMG sensor on the surface of a muscle [2]. A weak current signal generated as a surface EMG (sEMG) signal indicates muscle movement, changes in

the number of motor units, and their participation in activities. Moreover, activity patterns, metabolic status, and other factors can accurately reflect muscle activity state and functional status in real time. The study of muscle fatigue status based on sEMG signals was initially proposed in the 1980s [2], [3]. When muscle movement reaches the anaerobic threshold (AT), muscles demonstrate a fatigued status. The ventilation threshold (VT) is considered the gold standard for determining the AT [4]. Meanwhile, VT refers to the breakpoint during exercise at which ventilation starts to increase at a rate faster than that of oxygen uptake (VO2). VT is calculated with the V-slope method [4]. However, the VT measurement device is complex, expensive, and inconvenient. By contrast, an sEMG signal measurement device offers convenient testing and simple operation; thus, it is widely used in sports medicine.

However, sEMG signals obtained by existing acquisition technology contain certain noise, and sEMG signals must

The associate editor coordinating the review of this manuscript and approving it for publication was Jenny Mahoney.

be analyzed by professional neurologists to determine the state of muscle fatigue by examining the EMG waveform. In the process of training without the presence of experts, warning signs of muscle fatigue cannot be detected in time, and muscle injury accidents may occur. Thus, developing a method for the intelligent recognition of muscle fatigue based on sEMG signals is necessary. This method would rely on the EMG signal denoising method and muscle fatigue feature extraction and classification. In recent years, noise cancellation algorithms and automatic classification algorithms for sEMG signals were widely developed. Olivier Girard *et al.* used M-wave root mean square (RMS) changes to reflect the fatigue process of vastus lateralis (VL) and rectus femoris (RF) muscles under high temperatures and mild conditions [5]. Cote-Allard, Ulysse *et al.* employed raw EMG, spectrograms, and continuous wavelet transform as inputs of a deep learning network to classify sEMG signals [6]. H. Li *et al.* proposed a wavelet-based vibration signal denoising algorithm with a new adaptive threshold function to eliminate background noise effectively [7]. Meanwhile, A. Subasi *et al.* provided a method to visualize the onset of fatigue processes by separating myoelectric signals from fresh and fatigued muscles using neural networks in independent component analysis [8]. Xu Y. S. *et al.* investigated the effectiveness of a wavelet transform-domain filter for denoising EMG signals [9]. Moreover, Rachel L. Whittaker *et al.* constructed a linear regression model using quantitative perceptual fatigue scores and muscle fatigue accumulation [10]. Qi Wu *et al.* proposed a BFA-GSVCM classification method to solve the performance problem of the SVCM classifier by improving the loss function in the SVCM establishment process and compared it with the GSVCM, GA-GSVCM, PSO-SVCM, and other classification algorithms [11].

The support vector method proposed by Vapnik is an algorithm for the binary classification of data based on supervised learning [12]. Meanwhile, support vector machine (SVM) was developed from 1992 to 1995 based on statistical theory [13], [14]. Hubel and Wiesel [15] first proposed the concept of the convolutional neural network (CNN) in 1962; in 1998, LeCun *et al.* [16] established the first CNN model, namely, LeNet-5, to solve classification problems. Hinton and Salakhutdinov [17] advanced the CNN, thereby facilitating the development of other CNN network structures. The present study proposes an improved wavelet threshold function for sEMG signal denoising and combines the CNN and SVM to improve fatigue classification accuracy. The experimental results indicate that the algorithm proposed in this study has better performance in signal denoising and fatigue state classification than the algorithms used in previous research.

Two main contributions of this work can be summarized as follows:

1) A new wavelet threshold denoising method is used to eliminate the sEMG signal noise and motion noise in the sEMG signal and maintain the details of the sEMG signal.

2) The CNN-SVM classification algorithm is used to classify the time- and frequency-domain features of sEMG signals to accurately identify muscle fatigue status.

In our research, we aimed to accurately monitor the user's muscle fatigue status during exercise and reduce the risk of sports injuries. Such injuries are the main challenge for the implementation of exercise guidance.

II. METHODS

A. PARTICIPANTS

Fourteen healthy males ($n = 14$, age range: 20–30 years, height: 1.75 ± 0.1 m, weight: 67.5 ± 8.6 kg) and 6 healthy females ($n = 6$, age range: 20–30 years, height: 1.60 ± 0.05 m, weight: 52 ± 3.4 kg) were recruited for this study. All the participants were informed of the purpose, methodology, and potential risks of the study before their verbal and written informed consent was obtained. None of the participants reported cardiovascular diseases or muscular disorders. Moreover, some of the participants had certain training foundation.

B. PROCEDURES

The participants were instructed to refrain from high-intensity training, maintain a regular diet, and abstain from ingesting stimulants (caffeine, nicotine, and so on) or alcohol a day before the test. Each of the participants performed warm-up exercises for 2–3 min before the test. The protocol was 50 W as the initial workload, and a 25 W workload was added every 2 min for the progressive test phase. The participants were instructed to maintain a pedaling rate within the range of 60–70 rpm throughout the test. The test was terminated when a participant reached volitional fatigue and was unable to maintain a pedaling rate above 60 rpm.

C. DATA ACQUISITION

Throughout each exercise trial, pulmonary ventilation, VO2, and carbon dioxide (CO_2) were measured by using a portable gas analyzer (K4b2 Cosmed, Rome, Italy). Respiratory gas exchange measurements were obtained every 5 s. The regression analysis of the slope of CO_2 uptake versus the VO2 plot via the V-slope method was used to calculate the VT [18].

The participants' skin was prepared by shaving off excess hair and rubbing it with alcohol to reduce impedance. Subsequently, sEMG sensors were placed on five muscles on the left leg. The position of the sEMG sensors is shown in FIGURE 1. The sEMG sensors were fixed with a sports bandage, which would not affect the participants in executing the test protocol in the cycle ergometer. The EMG signals of the RF, VL, vastus medialis (VM), tibialis anterior (TA), and gastrocnemius (GA) muscles were detected by bipolar (20 mm center-to-center 1 cm × 1 cm in diameter) Ag–AgCl surface electrodes (Noraxon, USA).
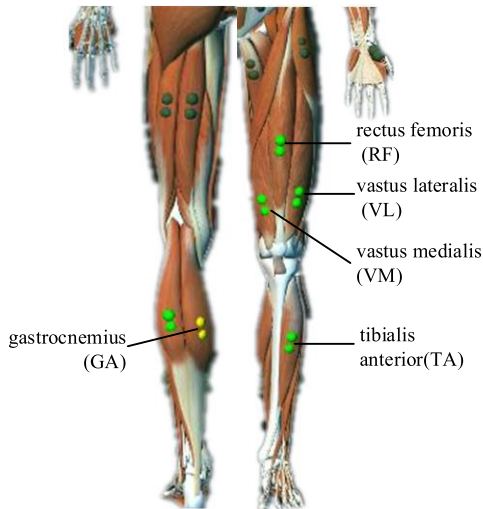
FIGURE 1. Description of muscle location on the left leg and sEMG electrode placement; GA, TA, RF, VM, and VL muscles.

D. sEMG SIGNAL DENOISING ANALYSIS

Noise is ubiquitous, and numerous noises can be detected in an EMG signal. Many data analysis methods were designed to eliminate noise and extract real signals from data. In 1988, Ingrid Daubechies first applied wavelet transform to signals for filtering [19]. French scientist Stephane Mallat proposed the main wavelet transform algorithm in the same year [20]. In the current research, the application of wavelet denoising algorithm was highly extensive. This algorithm is simple to implement and demonstrates remarkable denoising effect in practical applications. In general, the acquired EMG signals were composed of real signals and noise.

$$f(t) = s(t) + n(t) \quad (1)$$

where $f(t)$ is the acquired sEMG signals, and $s(t)$ and $n(t)$ represent real signals and noise, respectively. The wavelet coefficient $w_{j,k}$ obtained by wavelet transform decomposition on the original myoelectric signal $f(t)$ is composed of two parts, that is, the wavelet coefficient $u_{j,k}$ corresponding to $s(t)$ and the wavelet coefficient $v_{j,k}$ corresponding to $n(t)$. To achieve optimal performance in wavelet analysis, a suitable wavelet function should be employed. Most studies on sEMG analysis concluded that the Daubechies (Db) wavelet family is the most suitable wavelet for sEMG signal analysis [21]–[23]. We adopted the Db7 wavelet family as the wavelet basis following the recommendations of previous reports [24]–[26].

The steps of the wavelet threshold denoising method are as follows:

Step 1. Select the appropriate wavelet base and decomposition layer to perform wavelet decomposition on the acquired sEMG signals and obtain a set of wavelet coefficients $w_{j,k}$.

Step 2. Select the appropriate threshold function to process $\hat{w}_{j,k}$ to calculate the estimated wavelet coefficient $\hat{w}_{j,k}$.

Step 3. Inversely transform the processed wavelet coefficients to reconstruct the noise-canceled signal.

The method for choosing an appropriate threshold function in step 2 to make $||\hat{\omega}_{j,k} - u_{j,k}||$ as small as possible is controversial. If the threshold is too small, then it will not filter interference signals, resulting in no obvious denoising effect. By contrast, if the threshold is too large, then it will cause excessive signal loss, which will affect the signal analysis. Therefore, choosing the appropriate threshold function is crucial for sEMG signal denoising analysis. Commonly used threshold functions include hard threshold, soft threshold [27], and semi-threshold functions.

The hard threshold function is expressed as follows:

$$\hat{w}_{j,k} = \begin{cases} w_{j,k}, & |w_{j,k}| \geq \lambda \\ 0, & |w_{j,k}| < \lambda \end{cases} \quad (2)$$

The soft threshold function is expressed as follows:

$$\hat{w}_{j,k} = \begin{cases} \text{sign}(w_{j,k})(|w_{j,k}| - \lambda), & |w_{j,k}| \geq \lambda \\ 0, & |w_{j,k}| < \lambda \end{cases} \quad (3)$$

The Semi-threshold function is expressed as follows:

$$\hat{w}_{j,k} = \begin{cases} 0, & |w_{j,k}| \leq \lambda_1 \\ \text{sign}(w_{j,k})\dfrac{\lambda_2(|w_{j,k}| - \lambda_1)}{\lambda_2 - \lambda_1}, & \lambda_1 < |w_{j,k}| < \lambda_2 \\ w_{j,k}, & |w_{j,k}| > \lambda_2 \end{cases} \quad (4)$$

In Eqs. (2) and (3), $W_{j,k}$ is the wavelet coefficient, and λ is the threshold, as follows:

$$\lambda = \sigma (2 \log(N))^{1/2} \quad (5)$$

where N is the signal length, and σ is the variance of the noise:

$$\sigma = \frac{\text{MAD}_j}{0.6745} \quad (6)$$

where MAD_j is the median value of the wavelet decomposition coefficient of the j th layer [27]–[29].

Although widely used, hard threshold, soft threshold, and semi-threshold functions have several drawbacks. In Eq. (2), the threshold function is discontinuous when $w_{j,k} = \pm\lambda$, which causes oscillations during wavelet coefficient reconstruction, resulting in a poor denoising effect. The deviation between the estimated wavelet coefficient and actual wavelet coefficient in Eq. (3) cannot be eliminated, thereby causing poor approximation between the reconstructed signal and the real signal. In Eq. (4), two thresholds, that is, λ_1 and λ_2, must be estimated in the semi-threshold function, but doing so is difficult.

The improved threshold function proposed in this paper is as follows:

$$
\hat{w}_{j,k} = \begin{cases} w_{j,k} - \dfrac{m\lambda^{k+1}\text{sign}(w_{j,k})}{(m+1)\left|w_{j,k}\right|^{k}} + \dfrac{\lambda\text{sign}(w_{j,k})}{\left(w_{j,k}^{2} - \lambda^{2}\right)^{1/2}}, \\ \qquad\qquad\qquad \left|w_{j,k}\right| > \lambda \\ \dfrac{\text{sign}(w_{j,k})\left|w_{j,k}\right|^{k+1}}{(m+1)\lambda^{k}}, \\ \qquad\qquad\qquad \left|w_{j,k}\right| \le \lambda \end{cases} \tag{7}
$$

where m and k are variable parameters, $m \in [0, 1]$, and k is a positive integer. The improved threshold function is continuous and steerable at the $\pm\lambda$ point. Parameters m and k in the threshold function Eq. (5) are the adjustment factors. When $k \ge |\lambda|$ and $m \to 0$, the function has a hard threshold, whereas when $0 < k < |\lambda|$ and $m \to 1$, the function infinitely approaches the soft threshold. In the function, m adjusts the variation in the wavelet coefficient, and k adjusts the smoothness of the threshold function in $|W_{j,k} \le \lambda|$. The new threshold function proposed in this study combines the advantages of soft threshold, hard threshold, and semi-threshold functions. This approach enables the smooth transition of the wavelet threshold curve. The improved threshold function proposed in this study realizes the smooth transition of the wavelet threshold curve and avoids the pseudo-Gibbs phenomenon. Therefore, the reconstructed signal is smooth.

The threshold λ is the key to denoising sEMG signals. The threshold calculation method proposed by Grace *et al.* is not ideal for practical applications and can lead to oversegmentation [30]. As the number of sEMG signal layers decomposed by wavelets increases, noise energy gradually becomes weak, and the energy of real sEMG signals increases. The wavelet threshold is selected based on the high- and low-frequency characteristics of the signals.

The following hierarchical threshold estimation is obtained based on Eq. (8).

$$
\lambda = \sigma \left(2 \times \log(N)\right)^{1/2} g(j) \tag{8}
$$

$$
g(j) = \left[\dfrac{1}{4(2\pi)^{1/2}}\right] \exp\left(-\dfrac{j^2}{32}\right) \tag{9}
$$

where j is the number of wavelet decomposition levels. When we calculated the high-frequency threshold, g(j) was a large value, resulting in a slightly large threshold. However, when we calculated the low-frequency threshold, g(j) was a small value, resulting in a slightly small threshold [g(j) $\in$ (0,1)].

E. FEATURE EXTRACTION

The analysis of sEMG signals is concentrated in the time and frequency domains. In this study, the time- and frequency-domain features of the denoised sEMG signals were extracted. RMS and IEMG signal are generally used to describe changes in EMG amplitude during contraction fatigue. The mathematical expressions of RMS and IEMG

signal are shown as Eqs. (10) and (11).

$$
\text{IEMG} = \int_{t}^{t+T} |x(t)| \, dt \tag{10}
$$

$$
\text{RMS} = \left[\dfrac{1}{T}\int_{t}^{t+T} x^2(t)dt\right]^{1/2} \tag{11}
$$

Median frequency (MF) and mean power frequency (MPF) are commonly used to describe the frequency-domain characteristics of sEMG signals. The mathematical expressions of MF and MPF are shown as Eqs. (12) and (13).

$$
\int_{f_1}^{\text{MF}} \text{PS}(f)df = \int_{\text{MF}}^{f_2} \text{PS}(f)df \tag{12}
$$

$$
\text{MPF} = \dfrac{\int_{f_1}^{f_2} f \times \text{PS}(f)df}{\int_{f_1}^{f_2} \text{PS}(f)df} \tag{13}
$$

where PS is the power spectrum of the sEMG signal, which is calculated using the periodogram power spectral density estimate method, and f_1 and f_2 determine the frequency-domain signal bandwidth of the sEMG signal (f_1 = lowest frequency and f_2 = highest frequency of the bandwidth).

Band spectral entropy (BSE) is a method that combines information entropy and band decomposition for sEMG signal analysis. The calculation method for BSE is shown in Eqs. (14) and (15), where P_i is the spectral energy in the frequency band, and Pi is the normalized spectral energy.

$$
\text{BSE} = -\sum_{i=1}^{n} P_i \ln P_i \tag{14}
$$

$$
P_i = \dfrac{\sum_{i=1}^{n} E_i}{E} \tag{15}
$$

F. FATIGUE RECOGNITION

As a neural network algorithm, the CNN often requires a large number of training samples; thus, overfitting problems may emerge. SVM training with a large number of training samples; thus, overfitting problems may emerge. SVM training with a large number of training samples will consume substantial machine memory and computing time. The SVM based on statistical theory and structural risk minimization can solve the problems of small samples and overfitting. This study designed a suitable CNN-SVM model using manual design features to overcome the shortcomings of traditional classifier algorithms and improved the performance of the classifier. The fully connected layer of the CNN was replaced with the SVM, and the remaining convolutional layers and subsampling layers were used to extract features from the noise-reduced data automatically. Feature data were classified with the Gaussian kernel SVM algorithm.

The following procedure describes the CNN-SVM classification system for the fatigue status recognition of sEMG signals.

Step 1. Data preparation: The sEMG signals after the noise reduction process were used as the input sample of the CNN. The sample was divided into a training sample, a verification

sample, and a test sample in accordance with certain proportions.

Step 2. Training samples to train the CNN. Feature vectors corresponding to the training samples were extracted after training.

Step 3. The SVM was trained with the training sample feature vectors from step 2.

Step 4. In the test phase, the trained SVM was used to replace the fully connected layer of the CNN, and the test samples were inputted into the trained CNN to obtain the corresponding feature vector of each test sample.

Step 5. The feature vector of the test sample was trained for classification or regression.

The process of identifying muscle fatigue state based on the improved wavelet threshold and CNN-SVM is shown in Fig. 2.
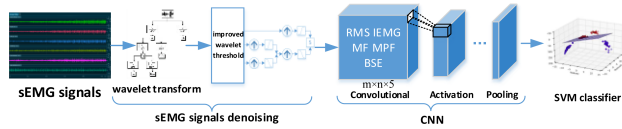

FIGURE 2. The process of realizing muscle fatigue state recognition based on improved wavelet threshold and CNN-SVM methods.

The Xavier method was used to randomly initialize the weight matrix (W) of two adjacent layers of the network following Eq. (16) [31], where n_j and n_{j+1} represent the number of neurons in the two adjacent layers. With reference to previous research [32], [33], a feature extractor consisting of two convolutions and pooling was designed to construct the CNN structure, and a fully connected layer of two layers of perceptrons was used to implement the classification function. The ReLU function (17) was employed as the activation function of the convolutional layer and fully connected layer.

$$W \sim U \left[-\frac{6^{1/2}}{(n_j+n_{j+1})^{1/2}}, \frac{6^{1/2}}{(n_j+n_{j+1})^{1/2}} \right] \quad (16)$$

$$f(x) = \begin{cases} x, & x > 0 \\ 0, & x \le 0 \end{cases} \quad (17)$$

The SVM identified fatigue state was based on the sEMG feature data extracted by the CNN. The kernel function of the SVM uses a Gaussian kernel function with satisfactory learning capability. Eq. (18) is an SVM classification decision function that identifies muscle fatigue, and Eq. (19) is the kernel function of the SVM.

$$f(x) = \text{sign} \left[\sum_{i=1}^{N} \alpha_i^* y_i K(x, z) + b^* \right] \quad (18)$$

$$K(x, z) = \exp \left(-\frac{\|x - z\|^2}{2\sigma^2} \right) \quad (19)$$

III. RESULTS
A. sEMG SIGNAL DENOISING EFFECT EVALUATION
The sEMG signals were recorded at a rate of 2000 Hz using wireless myoelectric sensors. Figure 3 presents the measured
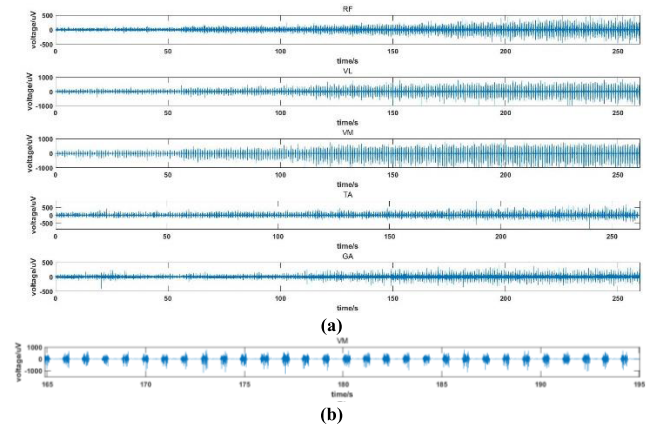

FIGURE 3. Measured sEMG signals from the participants.

sEMG signals from the participants. An increased amount of noise was detected in the original sEMG signals. The effectiveness of the improved wavelet threshold algorithm proposed in this study for denoising sEMG signals was verified by comparing traditional thresholding methods. Signal-to-noise ratio (SNR) and RMS error (RMSE) were used as the objective evaluation indicators.

$$\text{SNR} = 10 \log \left\{ \frac{\sum_n s(t)^2}{\sum_n [s(t) - \hat{s}(t)]^2} \right\} \quad (20)$$

$$\text{RMSE} = \left\{ \frac{\sum_n 10 \log [s(t) - \hat{s}(t)]^2}{N} \right\}^{1/2} \quad (21)$$

Hard threshold, soft threshold, semi threshold, the new wavelet threshold proposed by Zhang et al. [34], and the wavelet threshold algorithm proposed in this study were compared, and the results are shown in Table 1. The simulation experiment data in Table 1 indicate that the improved wavelet threshold denoising method proposed in this study achieved a large peak SNR and a small RMSE. Thus, the improved wavelet threshold denoising algorithm was a satisfactory denoising algorithm.

TABLE 1. Performance comparison of different noise reduction algorithms.

Denoising algorithm	SNR	RMSE
Hard-threshold	2.547	437
Soft-threshold	2.154	514
Semi-threshold	3.354	217
New threshold[34]	3.471	191
Improved threshold	3.658	182

B. FATIGUE STATE RECOGNITION
For muscle fatigue analysis, typical sEMG feature sets are in the time and frequency domains, of which the most common are RMS, IEMG signal, MPF, and MF. According to previous research, when muscles are fatigued, IEMG signal and

RMS will increase but MF and MPF will decrease. The recorded sEMG signals were divided into N time windows, and each window had a 1.5 s sEMG signal. The calculated RMS and IEMG signal of the sEMG signals demonstrated an increasing trend, as shown in Fig. 3. The RMS and IEMG signal of the sEMG signals of the RF, VL, and VM muscles exhibited a significant upward trend. Figures 4 and 5 show that MPF and MF decreased, and BSE initially increased and then decreased after the muscles entered the fatigued state. As revealed by the yellow line in Figs. 4(a) and 4(b), the slope of the MF fitting curve was –0.00898, and the slope of the MPF fitting curve was –0.00607. The MPF characteristic parameters showed a slight upward trend when muscle fatigue increased. The yellow line in Fig. 5 demonstrates that the slope of the BSE fitting curve was a cubic function.
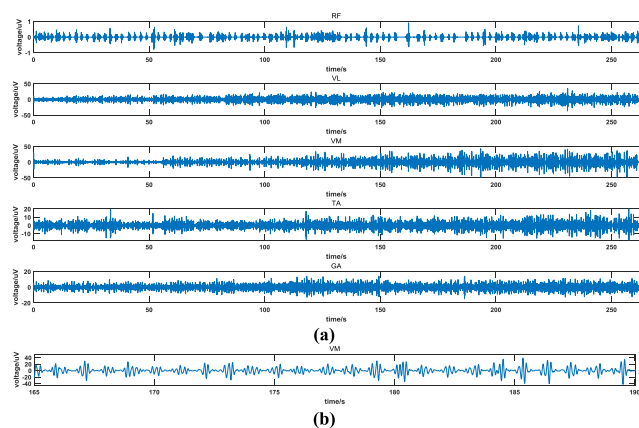

(a)

(b)

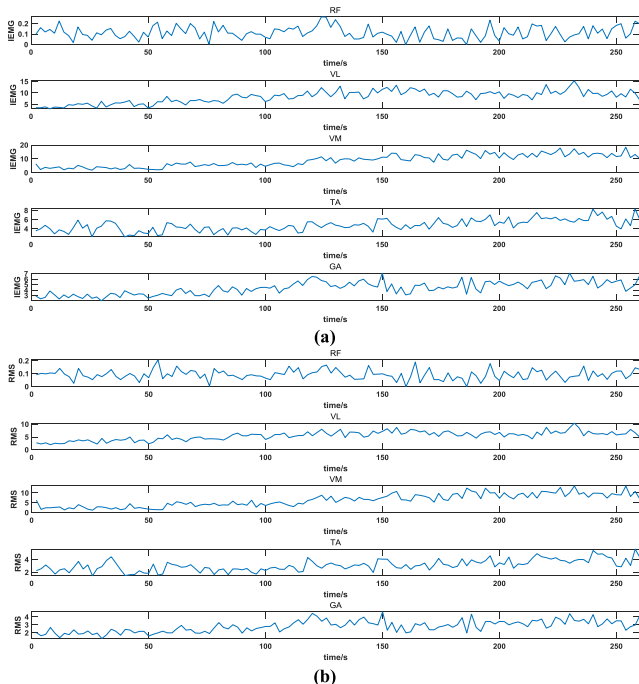**FIGURE 4.** Denoised sEMG signals.

(a)

(b)

FIGURE 5. Trend of instantaneous IEMG (a) and RMS(b) for participant.

To accurately represent classification accuracy, we selected the following scheme to confirm the effectivity of the proposed method among the 100 sEMG signal data samples from the 20 participants. The sEMG signals of the RF, VL, VM, TA, and GA muscles of the 20 participants during the fatigue test were divided into normal sEMG signals and fatigued sEMG signals on the basis of the time corresponding to the VT. The above feature types were divided into two categories, where 0 represented a normal status, and 1 represented a fatigued status. The 2D data obtained by combining RMS, IEMG, MF, MPF, and BSE with the muscle fatigue status values were used as the input samples of the CNN, SVM, PSO-SVM, and CNN-SVM. For the CNN-SVM-based classification, the hyperparameters included kernel size (5×5), pool size (2×2), and activation function (ReLU). The number of training epochs was dependent on the data, which to be between 15 and 32 epochs in the pre-training process and less than 10 in the fine-tuning process. The size of the filter in the network was optimized by gradually decreasing from a large number. The number of filters in the first CNN was large, and all steps were set to 1. The AdaDelta optimizer with a 2–5 learning rate and a decay rate of 10–4 yielded the lowest loss in all dataset permutations. We used grid search to optimize the CNN model and stopped training early when the verification loss was no longer improved.

All algorithms were implemented in MATLAB R2018a. Theoretically, the program running time of the CNN-SVM algorithm was significantly higher than that of the PSO-SVM and SVM algorithms. The simulation time of the CNN-SVM algorithm was 13757 s. By contrast, the simulation times of the CNN, PSO-SVM, and SVM algorithms were 12630, 10972, and 9237 s, respectively.

For each test data set, we used 10-fold cross-validation to train a supervised classifier. Eightfold validation was used in training. One of them was used as a validation set to optimize the network. The last fold was used to test the algorithm. In the results, only muscle fatigue state and non-fatigue state were predicted. The classification accuracy of the CNN-SVM algorithm was compared with that of the SVM and PSO-SVM algorithms, and the results are shown in Table 1. By comparing the fatigue classification accuracy of the four algorithms on the feature data sets of three different combinations, we found that the CNN-SVM classification mode was better than the three other algorithms. The experimental results of this study proved that the BSE of sEMG signals proposed by Liu *et al.* [35] can be classified as a feature type, and classification accuracy can be improved. Table 3 shows the comparison of the influence of the three denoising algorithms on the accuracy of four classification algorithms.

Fig. 8 presents the training and validation losses of the CNN-SVM model by epochs. By contrast, both the training and validation losses decreased steadily for the CNN-SVM model, which also indicated that the data overfitting problem was alleviated.
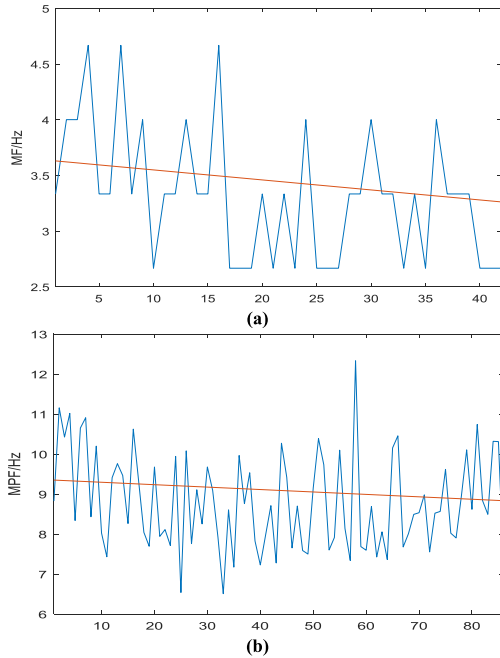
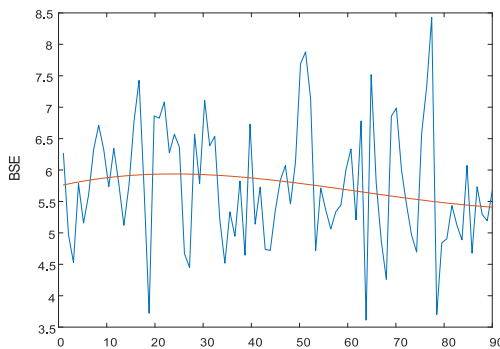**FIGURE 6.** Trend of MF(a) and MPF(b) for participant.

FIGURE 7. Trend of BSE for participant.

FIGURE 8. Mean training loss and mean validation loss for CNN-SVM.

IV. DISCUSSION

The purpose of the present study was to propose a method that could effectively remove noise in sEMG signals and accurately detect muscle fatigue. The improved wavelet threshold denoising algorithm proposed in this study performed better than the traditional wavelet threshold algorithm for sEMG signal denoising. We compared and evaluated the

TABLE 2. Comparison of the classification accuracy(in %) of different feature types by SVM, PSO-SVM, CNN, CNN-SVM classification algorithms.

Feature	SVM	PSO-SVM	CNN	CNN-SVM
RMS,IEMG	70.33±2.73	72.14±0.84	70.14±2.12	74.45±0.07
RMS,IEMG, MPF,MF	71.84±1.53	72.72±1.88	74.22±1.66	79.82±1.62
RMS,IEMG, MPF,MF,BSE	73.21±2.84	76.89±1.45	78.86±2.27	83.51±3.18

TABLE 3. Compare fatigue classification accuracy(in%) based on the combination of denoising algorithm and classification algorithm.

Denoising algorithm	SVM	PSO-SVM	CNN	CNN-SVM
Semi-threshold	68.11±2.07	71.47±0.18	71.64±2.03	76.19±1.66
New threshold[34]	72.87±1.77	70.74±3.51	76.14±1.75	82.89±2.31
Improved threshold	73.21±2.84	76.89±1.45	78.86±2.27	83.51±3.18

classification performance of the CNN-SVM, SVM, and PSO-SVM algorithms for sEMG signal fatigue status.

Typical sEMG features for muscle fatigue analysis are concentrated in the time and frequency domains [36], [37]. To characterize the frequency domain of sEMG, researchers often use MF and MPF [38]. During sEMG time-domain analysis, researchers often use RMS and IEMG [39]. As the muscles of the participants became fatigued, the changes in the characteristics of the EMG signal parameters of the subjects were basically the same, and they were repeatable. According to related research, IEMG and RMS values increase, and MPF values decrease [40]–[42]. Different positions of the collected EMG signals will lead to varying trends in MPF. In Hogrel *et al.*'s study, the MPF parameters of the sEMG signals extracted from the lateral femoral (LF) indicated a regular downward trend followed by an upward trend as the LF gradually entered the fatigue status during the test [43]. The experimental results in this study were consistent with previous work, but the characteristics of some participants did not change significantly. The feature types of RMS + IEMG + MF + MPF + BSE used in this study solved the problem that a single feature description of muscle fatigue characteristics was not sufficiently reliable. The addition of BSE features based on the traditional time- and frequency-domain features further improved the accuracy of muscle fatigue classification. Previous research indicated that SVM and PSO-SVM algorithms have improved classification accuracy for feature types (RMS + IEMG + MF + MPF + BSE) [44]. The classification accuracy of CNN-SVM for muscle fatigue state were 7.48%, 7.33%, and 7.01% higher than SVM, PSO-SVM, and CNN, respectively. The improved wavelet threshold denoising algorithm proposed in this paper was better

than the semi-threshold and new threshold denoising algorithm in improving the classification accuracy of different classification algorithms. To improve classification accuracy, the improved wavelet threshold algorithm was 8.36%–11.35% higher than the semi-threshold algorithm and 1.75%–5.51% higher than the new algorithm.

Muscle fatigue, particularly when undetected, can increase the risk of injury. Identifying muscle fatigue based on sEMG signals is necessary and can serve as the foundation of automated systems. Automated muscle fatigue detection/prediction technology through wearable devices could play an essential role in the design of training assistance systems.

V. CONCLUSION

This study proposes a method that can obtain real sEMG signals and accurately identify muscle fatigue. The improved wavelet denoising algorithm proposed in this study demonstrates better performance than traditional wavelet threshold denoising algorithms for denoising sEMG signals. The extraction of RMS, IEMG signal, MF, MPF, and BSE features from denoised sEMG signals to use as input of the CNN-SVM algorithm achieves accurate fatigue status recognition. The improved wavelet algorithm can improve the accuracy of the classification algorithm to identify muscle fatigue status. Although some features do not change significantly under muscle fatigue, comprehensive comparison results indicate that the CNN-SVM algorithm exhibits satisfactory performance in muscle fatigue recognition. The accuracy of mean instantaneous frequency based on ensemble empirical mode decomposition–Hilbert transform for the CNN-SVM algorithm to identify muscle fatigue status will be further explored in future research.

REFERENCES

[1] B. Bigland-Ritchie and J. J. Woods, "Changes in muscle contractile properties and neural control during human muscular fatigue," *Muscle Nerve*, vol. 7, no. 9, pp. 691–699, Dec. 1984.

[2] H. A. Devries, T. Moritani, A. Nagata, and K. Magnussen, "The relation between critical power and neuromuscular fatigue as estimated from electromyographic data," *Ergonomics*, vol. 25, no. 9, pp. 783–791, Sep. 1982.

[3] H. A. Devries, M. W. Tichy, T. J. Housh, K. D. Smyth, A. M. Tichy, and D. J. Housh, "A method for estimating physical working capacity at the fatigue threshold (PWCFT)," *Ergonomics*, vol. 30, no. 8, pp. 1195–1204, Aug. 1987.

[4] W. L. Beaver, K. Wasserman, and B. J. Whipp, "A new method for detecting anaerobic threshold by gas exchange," *J. Appl. Physiol.*, vol. 60, no. 6, pp. 2020–2027, Jun. 1986.

[5] O. Girard, D. J. Bishop, and S. Racinais, "M-wave normalization of EMG signal to investigate heat stress and fatigue," *J. Sci. Med. Sport*, vol. 21, no. 5, pp. 518–524, May 2018.

[6] U. Cote-Allard, C. L. Fall, A. Drouin, A. Campeau-Lecours, C. Gosselin, K. Glette, F. Laviolette, and B. Gosselin, "Deep learning for electromyographic hand gesture signal classification using transfer learning," *IEEE Trans. Neural Syst. Rehabil. Eng.*, vol. 27, no. 4, pp. 760–771, Apr. 2019.

[7] H. Li, Y. Zhou, F. Tian, S. Li, and T. Sun, "Wavelet-based vibration signal de-noising algorithm with a new adaptive threshold function," *Chin. J. Sci. Instrum.*, vol. 36, no. 10, pp. 2200–2206, 2015.

[8] A. Subasi and M. K. Kiymik, "Muscle fatigue detection in EMG using time–frequency methods, ICA and neural networks," *J. Med. Syst.*, vol. 34, no. 4, pp. 777–785, Aug. 2010.

[9] Y. Xu, J. B. Weaver, D. M. Healy, and J. Lu, "Wavelet transform domain filters: A spatially selective noise filtration technique," *IEEE Trans. Image Process.*, vol. 3, no. 6, pp. 747–758, 1994.

[10] R. L. Whittaker, M. W. Sonne, and J. R. Potvin, "Ratings of perceived fatigue predict fatigue induced declines in muscle strength during tasks with different distributions of effort and recovery," *J. Electromyogr. Kinesiol.*, vol. 47, pp. 88–95, Aug. 2019.

[11] Q. Wu, C. Xi, L. Ding, C. Wei, H. Ren, R. Law, H. Dong, and X. L. Li, "Classification of EMG signals by BFA-optimized GSVCM for diagnosis of fatigue status," *IEEE Trans. Autom. Sci. Eng.*, vol. 14, no. 2, pp. 915–930, Apr. 2017.

[12] V. Vapnik, *The Nature of Statistical Learning Theory*. New York, NY, USA: Springer, 1995.

[13] C. Cortes and V. Vapnik, "Support-vector network," *Mach. Learn.*, vol. 20, no. 3, pp. 273–297, 1995.

[14] B. E. Boser, I. M. Guyon, and V. N. Vapnik, "A training algorithm for optimal margin classifiers," in *Proc. 5th Annu. workshop Comput. Learn. Theory (COLT)*, Pittsburgh, PA, USA, 1992, pp. 144–152.

[15] D. H. Hubel and T. N. Wiesel, "Receptive fields, binocular interaction and functional architecture in the cat's visual cortex," *J. Physiol.*, vol. 160, no. 1, pp. 106–154, Jan. 1962.

[16] Y. Lecun, L. Bottou, Y. Bengio, and P. Haffner, "Gradient-based learning applied to document recognition," *Proc. IEEE*, vol. 86, no. 11, pp. 2278–2324, 1998.

[17] G. E. Hinton, "Reducing the dimensionality of data with neural networks," *Science*, vol. 313, no. 5786, pp. 504–507, Jul. 2006.

[18] W. L. Beaver, K. Wasserman, and B. J. Whipp, "A new method for detecting anaerobic threshold by gas exchange," *J. Appl. Physiol.*, vol. 60, no. 6, pp. 2020–2027, Jun. 1986.

[19] I. Daubechies, "Orthonormal bases of compactly supported wavelets," *Commun. Pure Appl. Math.*, vol. 41, no. 7, pp. 909–996, Oct. 1988.

[20] S. G. Mallat, "A theory for multiresolution signal decomposition: The wavelet representation," *IEEE Trans. Pattern Anal. Mach. Intell.*, vol. 11, no. 7, pp. 674–693, Jul. 1989.

[21] M. S. Hussain, M. B. I. Reaz, F. Mohd-Yasin, and M. I. Ibrahimy, "Electromyography signal analysis using wavelet transform and higher order statistics to determine muscle contraction," *Expert Syst.*, vol. 26, no. 1, pp. 35–48, Feb. 2009.

[22] K. Mahaphonchaikul, D. Sueaseenak, C. Pintavirooj, M. Sangworasil, and S. Tungjitkusolmun, "EMG signal feature extraction based on wavelet transform," in *Proc. 7th Int. Conf. Electr. Eng./Electron., Comput., Telecommun.*, vol. 1, 2010, pp. 356–360.

[23] A. Phinyomark, C. Limsakul, and P. Phukpattaranont, "An optimal wavelet functions in wavelet denoising for multifunction myoelectric control," *ECTI Trans. Electr. Eng. Electron. Commun.*, vol. 8, no. 1, pp. 43–52, 2010.

[24] C.-F. Jiang, Y.-C. Lin, and N.-Y. Yu, "Multi-scale surface electromyography modeling to identify changes in neuromuscular activation with myofascial pain," *IEEE Trans. Neural Syst. Rehabil. Eng.*, vol. 21, no. 1, pp. 88–95, Jan. 2013.

[25] A. Phinyomark, A. Nuidod, P. Phukpattaranont, and C. Limsakul, "Feature extraction and reduction of wavelet transform coefficients for EMG pattern classification," *Electron. Electr. Eng.*, vol. 122, no. 6, pp. 27–32, Jun. 2012.

[26] M. Schimmack and P. Mercorelli, "An on-line orthogonal wavelet denoising algorithm for high-resolution surface scans," *J. Franklin Inst.*, vol. 355, no. 18, pp. 9245–9270, Dec. 2018.

[27] D. L. Donoho, "De-noising by soft-thresholding," *IEEE Trans. Inf. Theory*, vol. 41, no. 3, pp. 613–627, May 1995.

[28] D. O. Trad and J. M. Travassos, "Wavelet filtering of magnetotelluric data," *Geophysics*, vol. 65, no. 2, pp. 482–491, Mar. 2000.

[29] J. Lin, M. Y. Fu, and D. P. Li, "Self-adaptive wavelet threshold de-noising method and its application in image processing," *Acta Armamentar II*, vol. 32, no. 7, pp. 896–900, 2011.

[30] S. C. Y. Grace Bin and M. Vetterli, "Adaptive wavelet thresholding for image denoising and compression," *IEEE Trans. Image Process.*, vol. 9, no. 9, pp. 1532–1546, Sep. 2000.

[31] X. Glorot and Y. Bengio, "Understanding the difficulty of training deep feedforward neural networks," *Proc. 13th Int. Conf. Artif. Intell. Statist.*, Sardinia, Italy, 2010, pp. 249–256.

[32] S. Kiranyaz, T. Ince, and M. Gabbouj, "Real-time patient-specific ECG classification by 1-D convolutional neural networks," *IEEE Trans. Biomed. Eng.*, vol. 63, no. 3, pp. 664–675, Mar. 2016.

[33] J. Yang, M. N. Nguyen, P. P. San, X. Li, and S. Krishnaswamy, "Deep convolutional neural networks on multichannel time series for human activity recognition," in *Proc. IJCAI AAAI Press*, 2015, pp. 3995–4001.

[34] Y. Zhang, W. Ding, Z. Pan, and J. Qin, "Improved wavelet threshold for image de-noising," *Frontiers Neurosci.*, vol. 13, pp. 1–7, Feb. 2019.

[35] J. Liu, R. Zou, D. Zhang, X. Xu, and X. Hu, "Analysis of the muscle fatigue based on band spectrum entropy of multi-channel surface electromyography," *J. Biomed. Eng.*, vol. 33, no. 3, pp. 431–435, 2016.

[36] K. Wang, "Conventional time-frequency method of sEMG and strategy used for dynamic muscle fatigue analysis," *Chin. J. Sports Med.*, vol. 29, no. 1, pp. 104–108, 2010.

[37] J. Duchêne and F. Goubel, "Surface electromyogram during voluntary contraction: Processing tools and relation to physiological events," *Crit. Rev. Biomed. Eng.*, vol. 21, no. 4, pp. 313–397, 1993.

[38] F. B. Stulen and C. J. De Luca, "Frequency parameters of the myoelectric signal as a measure of muscle conduction velocity," *IEEE Trans. Biomed. Eng.*, vol. BME-28, no. 7, pp. 515–523, Jul. 1981.

[39] D. Tkach, H. Huang, and T. A. Kuiken, "Study of stability of time-domain features for electromyographic pattern recognition," *J. Neuroengineering Rehabil.*, vol. 7, no. 1, pp. 21–34, 2010.

[40] A. Subasi and M. K. Kiymik, "Muscle fatigue detection in EMG using Time–Frequency methods, ICA and neural networks," *J. Med. Syst.*, vol. 34, no. 4, pp. 777–785, Aug. 2010.

[41] A. Georgakis, L. K. Stergioulas, and G. Giakas, "Fatigue analysis of the surface EMG signal in isometric constant force contractions using the averaged instantaneous frequency," *IEEE Trans. Biomed. Eng.*, vol. 50, no. 2, pp. 262–265, Feb. 2003.

[42] F. B. Stulen and C. J. De Luca, "Frequency parameters of the myoelectric signal as a measure of muscle conduction velocity," *IEEE Trans. Biomed. Eng.*, vol. BME-28, no. 7, pp. 515–523, Jul. 1981.

[43] J.-Y. Hogrel, J. Duchêne, and J.-F. Marini, "Variability of some SEMG parameter estimates with electrode location," *J. Electromyogr. Kinesiol.*, vol. 8, no. 5, pp. 305–315, Oct. 1998.

[44] C. Ang et al., "Muscle fatigue state classification system based on surface electromyography signal," *J. Comput. Appl.*, vol. 38, no. 6, pp. 1801–1808, 2018.

JUNHONG WANG received the B.Eng. degree in software engineering and electrical engineering automation from the East of China Jiaotong University, Nanchang, China, in 2014, and the M.Eng. degree from Anhui Engineering University, Wuhu, China in 2016. He is currently pursuing the Ph.D. degree in detection technology and automation with the University of Science and Technology of China, Hefei, China.

His main research interests include artificial intelligence and sports medicine.

YINING SUN received the B.S. degree in computer application from the University of Science and Technology of China, Hefei, China, and the Ph.D. degree in electronic engineering from the University of Rome, Rome, Italy.

He is currently a Professor with the University of Science and Technology of China. His research interests include exercise physiology and sensor technology.

SHAOMING SUN received the B.S. degree in mechanical automation from Jilin University, Jilin, China, in 2004, and the Ph.D. degree in agricultural mechanization and its automation from Jilin University, Jilin, China, in 2008.

His main research interests include exercise physiology and bio-robot.

• • •